RESEARCH ARTICLE

A Severity-Agnostic Atrophy Pattern in Spinocerebellar Ataxia Type 3: Volumetrics from ENIGMA-Ataxia

Jason W. Robertson, PhD,[1] Isaac Adanyeguh, PhD,[2] David J. Arpin, PhD,[3] Tetsuo Ashizawa, MD,[4] Benjamin Bender, PhD,[5] Fernando Cendes, MD, PhD,[6,7] Xi Chen, MSc,[8] Giulia Coarelli, MD, PhD,[9] Léo Coutinho, MD,[10] Andreas Deistung, PhD,[11] Imis Dogan, PhD,[12,13] Alexandra Durr, MD, PhD,[9] Jennifer Faber, MD, PhD,[14,15,16] for the ESMI MR Study Group, Juan Fernandez-Ruiz, PhD,[17] Mónica Ferreira, MSc,[14,18] Marcondes C. França, MD, PhD,[6,7] Sophia L. Göricke, MD,[19,20] Shuo Han, PhD,[21] Thomas Klockgether, MD, PhD,[14] Chen Liu, PhD,[8] Jun Luo, MSc,[8] Alberto R.M. Martinez, MD, PhD,[6,7] Sergio E. Ono, MD, PhD,[22] Chiadi U. Onyike, MD,[23] Gülin Öz, PhD,[2] for the EUROSCA MR Study Group, Henry Paulson, MD,[24] Jerry L. Prince, PhD,[25] Kathrin Reetz, MD,[12,13] Thiago J.R. Rezende, PhD,[6,7] Matthis Synofzik, MD,[26,27] Hélio A. Ghizoni Teive, MD, PhD,[10,28] Sophia I. Thomopoulos, BA,[29] Paul M. Thompson, PhD,[29] Dagmar Timmann, MD,[19,30] David Vaillancourt, PhD,[3,31,32] Bart van de Warrenburg, MD, PhD,[33] Judith van Gaalen, MD,[33,34] Xingang Wang, MSc,[8] Philipp Wegner, MSc,[14,18] Sarah H. Ying, MD,[35] Ian H. Harding, PhD,[36,37] and Carlos R. Hernandez-Castillo, PhD[1*]

Background: Spinocerebellar ataxia type 3 (SCA3) is a rare, inherited neurodegenerative disease characterized by progressive loss of motor coordination.

Objectives: We undertook a multisite magnetic resonance imaging study to profile the spatial spread of atrophy across the brain, determine whether atrophy preferentially maps onto specific functional networks, and investigate the relationship between cerebellar and cerebral atrophy.

Methods: Whole-brain grey and white matter (GM and WM) voxel-based morphometry was performed on 408 individuals with SCA3 (82 pre-ataxic) and 293 controls. The SCA3 cohort was stratified by ataxia severity to study progression. Cerebellar GM atrophy was mapped onto a task-based functional atlas. Cerebrocerebellar volumetric covariance was assessed to determine whether cerebral and cerebellar atrophy were coupled.

Results: The atrophy pattern is spatially consistent but progressive in magnitude across the disease course. The greatest atrophy (Cohen's $d > 1.5$) occurred in the pons, cerebellar WM, and cerebellar peduncles; correlations with ataxia severity and duration were also strongest ($-0.4 > r > -0.65$) in those regions. Cerebellar GM

[1]Faculty of Computer Science, Dalhousie University, Halifax, Nova Scotia, Canada; [2]Department of Radiology, Center for Magnetic Resonance Research, University of Minnesota Medical School, Minneapolis, Minnesota, USA; [3]Department of Applied Physiology & Kinesiology, University of Florida, Gainesville, Florida, USA; [4]Department of Neurology, Weill Cornell Medicine at Houston Methodist Research Institute, Houston, Texas, USA; [5]Department of Diagnostic and Interventional Neuroradiology, University Hospital Tübingen, Tübingen, Germany; [6]Department of Neurology, School of Medical Sciences, University of Campinas, Campinas, Brazil; [7]Brazilian Institute of Neuroscience and Neurotechnology (BRAINN), School of Medical Sciences, University of Campinas, Campinas, Brazil; [8]7T Magnetic Resonance Imaging Translational Medical Center, Department of Radiology, Southwest Hospital, Army Medical University (Third Military Medical University), Chongqing, China; [9]Sorbonne Université, Paris Brain Institute (ICM), Pitié-Salpêtrière Hospital, AP-HP, INSERM, CNRS, University Hospital Pitié-Salpêtrière, Paris, France; [10]Post-Graduate Program of Internal Medicine, Internal Medicine Department, Hospital de Clínicas, Federal University of Paraná, Curitiba, Brazil; [11]Department for Radiation Medicine, University Clinic and Outpatient Clinic for Radiology, University Hospital Halle (Saale), University Medicine Halle, Halle (Saale), Germany; [12]Department of Neurology, RWTH Aachen University, Aachen, Germany; [13]JARA-BRAIN Institute Molecular Neuroscience and Neuroimaging, Research Center Jülich GmbH, Jülich, Germany; [14]German Center for Neurodegenerative Diseases (DZNE), Bonn, Germany; [15]Department of Parkinson's Disease, Sleep and Movement Disorders, Center of Neurology, University Hospital Bonn, Bonn, Germany; [16]Department of Neuroradiology, University Hospital Bonn, Bonn, Germany; [17]Neuropsychology Laboratory, Department of Physiology, Faculty of Medicine, National Autonomous University of Mexico, Mexico City, Mexico; [18]Department of Neuroradiology, University of Bonn, Bonn, Germany; [19]Center for Translational Neuro- and Behavioral Sciences (C-TNBS), Essen University Hospital, University of Duisburg-Essen, Essen, Germany; [20]Institute of Diagnostic and Interventional Radiology and Neuroradiology, Essen University Hospital, University of Duisburg-Essen, Essen, Germany; [21]Department of Biomedical Engineering, Johns Hopkins University, Baltimore, Maryland, USA; [22]Clínica DAPI-Diagnóstico Avançado Por Imagem, Curitiba, Brazil; [23]Department of Psychiatry and Behavioral Sciences, Johns Hopkins University, Baltimore, Maryland, USA; [24]Department of Neurology, University of Michigan, Ann Arbor, Michigan, USA; [25]Department of Electrical and Computer Engineering, Johns Hopkins University, Baltimore, Maryland, USA; [26]Department of Neurodegenerative Diseases, Hertie Institute for Clinical Brain Research, Tübingen, Germany; [27]German Center for Neurodegenerative Diseases (DZNE), Tübingen, Germany; [28]Movement Disorders Unit, Neurology Service, Internal Medicine Department, Hospital de Clínicas, Federal University of Paraná, Curitiba, Brazil; [29]Imaging Genetics Center, Mark and Mary Stevens Institute for Neuroimaging and Informatics, Keck School of Medicine, University of Southern California, Marina del Rey, California, USA; [30]Department of Neurology, Essen University Hospital, University of Duisburg-Essen, Essen, Germany; [31]Department of Neurology, University of Florida, Gainesville,

atrophy was greatest ($d \cong 0.7$) in functional regions associated with motor planning/execution, attention, and emotional processing. Sparse cerebral cortical atrophy appears only in the most severe disease subgroup, while striatal atrophy begins in the earliest stages but does not worsen with increasing clinical severity. Reduced cerebrocerebellar volumetric covariance is observed in SCA3 participants versus controls.

Conclusions: Cerebellar and brainstem atrophy underlies greater ataxia severity in SCA3, but the spatial pattern of structural changes remains relatively consistent across the course of the disease. Cerebellar GM atrophy is spatially non-uniform, and occurs maximally in regions consistent with the motor and cognitive clinical presentation of SCA3. Cerebellar atrophy is not mirrored by corresponding cerebral structural changes.

Key Words: Cerebrocerebellar connectivity; Functional brain networks; Neurodegeneration; Spinocerebellar Ataxia; Voxel-based morphometry

Spinocerebellar ataxia type 3 (SCA3) is a neurodegenerative disease caused by a CAG triplet repeat expansion in the *ATXN3* gene,[1] resulting in misfolding and aggregation of the ataxin-3 protein.[2] This in turn results in neuronal cell death and/or demyelination in the spinal cord, cerebellum, brainstem, striatum, and thalamus, as well as in the tracts that link these structures.[1-3] SCA3 is defined by progressive cerebellar ataxia, and variable expression of neurological symptoms including peripheral neuropathy, bradykinesia, tremor, Parkinsonism, oculomotor impairment, and dysphagia.[1,4,5]

Non-invasive imaging techniques such as magnetic resonance imaging (MRI) have been crucial to describing the neuroanatomical changes underlying SCA3 and their relationship with clinical disease severity. A growing body of MRI research has examined the progression of SCA3 both longitudinally[6-11] and cross-sectionally.[9,12-15] This research indicates that regional atrophy is progressive in both spatial extent and severity, including an evolving pattern of infratentorial-to-cerebral atrophy[13] and distinct time courses of volume loss in cerebellar, brainstem, and striatal structures.[12] The extent of atrophy in key brain regions is correlated with motor impairment severity,[11,12,14,16] and symptoms consistent with cerebellar cognitive affective syndrome (CCAS).[14,17-19]

Florida, USA; [32]Norman Fixel Institute for Neurological Diseases, University of Florida, Gainesville, Florida, USA; [33]Department of Neurology, Donders Institute for Brain, Cognition, and Behaviour, Radboud University Medical Center, Nijmegen, The Netherlands; [34]Department of Neurology, Rijnstate Hospital, Arnhem, The Netherlands; [35]Department of Radiology, Johns Hopkins University, Baltimore, Maryland, USA; [36]QIMR Berghofer Medical Research Institute, Brisbane, Queensland, Australia; [37]School of Translational Medicine, Monash University, Melbourne, Victoria, Australia

***Correspondence to:** Prof. Carlos R. Hernandez-Castillo, Dalhousie University, 6050 University Ave, Halifax, Nova Scotia, B3H 4R2, Canada; E-mail: carlos.hernandez@dal.ca

Ian H. Harding and Carlos R. Hernandez-Castillo contributed equally to this study.

Funding agencies: This work was supported by the following grants and granting agencies: the Natural Sciences and Engineering Research Council of Canada (NSERC) grant RGPIN-2022-034638; Canada Research Chair grant CRC-2020-00079; the Advanced Clinician Scientist Programme (ACCENT), funding code 01EO2107; the German Federal Ministry of Education and Research (BMBF); the Australian National Health and Medical Research Council (Ideas Grant 1184403 and Investigator Grant 2026191); EU Joint Programme Neurodegenerative Disease Research (JPND); European Reference Network for Rare Neurological Diseases (ERN-RND); National Ataxia Foundation Clinical Research Consortium grant; National Science Foundation grant #EEC-1460674; National Institute of Health/National Institute of Neurological Disorders and Stroke grants R01NS056307, R01NS080816, and U01 NS104326; Johns Hopkins Institute for Clinical and Translational Research support from NIH National Center for Advancing Translational Sciences (NIH/NCATS) grant UL1TR001079; the Jane Tanger Black Fund for Young-Onset Dementia Research; the Netherlands Organisation for Health Research and Development; Foundation for Science and Technology, Portugal; Medical Research Council, Portugal; Regional Fund for Science and Technology, Azores; Servier; the National Ataxia Foundation; ZonMw grant 733051066; Friedreich's Ataxia Research Alliance (FARA) grant 92,133; São Paulo Research Foundation (FAPESP) grant 2013/07559-3 through CEPID/BRAINN; National Natural Science Foundation of China grant 82071910; Senior Medical Talents Program of Chongqing for Young and Middle-Aged grant 514Z395; Young and Middle-Aged Senior Medical Talents Studio of Chongqing grant 524Z28921; Excellent Young Talent Fund of the First Affiliated Hospital of the Army Medical University grant 2024YQBJ-2; German Research Foundation (DFG) grants DE 2516/1-1 and TI 239/17-1; National Council of Science and Technology of Mexico (CONACYT) grant A1-S-10669; General Directorate of Academic Personnel Affairs Support Program for Research and Technological Innovation Projects (DGAPA-PAPIIT) grant IN208625; the Gossweiler Foundation; NIH Big Data to Knowledge (BD2K) award U54 EB020403; and NIH grants R01MH123163, R01MH121246, and R01MH116147. For a complete list of ENIGMA-related grant support please see http://enigma.ini.usc.edu/about-2/funding/.

Relevant conflicts of interest/financial disclosures: J.F. received consultancy honoraria from Vico Therapeutics. T.K. received consultancy honoraria from Arrowhead, Bristol Myers Squibb, and UCB. Collaborating author Paola Giunti has received grants and honoraria for advisory board from Vico Therapeutics, honoraria for advisory board from Triplet Therapeutics, grants and personal fees from Reata Pharmaceutical, and grants from Wave.

Received: 31 October 2025; **Revised:** 27 March 2026; **Accepted:** 16 April 2026

Published online 11 May 2026 in Wiley Online Library (wileyonlinelibrary.com). DOI: 10.1002/mds.70349

Understanding the development of SCA3 in both time and space is critical for predicting clinical variability and progression, selecting imaging biomarkers for clinical translation, and targeting treatments. While many studies have undertaken these tasks by examining large anatomical regions of interest (ROIs),[11,12,15,20,21] voxel-based approaches can provide greater spatial specificity in the atrophy patterns underlying disease expression and progression.[22-25]

This study expands on the existing knowledge base using MRI data from a large, retrospective, multisite cohort of individuals with SCA3 spanning a broad spectrum of disease severity, including pre-ataxic individuals. Using voxel-based morphometry (VBM), we first established a profile of whole-brain atrophy in participants with SCA3 at different stages of ataxia severity. We then examined how the SCA3 atrophy pattern maps onto a functionally derived parcellation of the cerebellum.[26] Finally, we evaluated the relationship between cerebellar and cerebral atrophy using corticocerebellar covariance analysis to determine whether there is direct correspondence between volume loss in the cerebrum and cerebellum.

Methods

Participants and Data

This study used a retrospective, cross-sectional design with data aggregated through the ENIGMA-Ataxia working group. All procedures were approved by both the Monash University Human Research and Ethics Committee and the Dalhousie University Research Ethics Board. Structural MRI, demographics, and clinical data were collected from participants with SCA3 ($n = 408$) and healthy controls (CONT; $n = 293$) from 11 sites (Aachen, Germany; Baltimore, USA; Campinas, Brazil; Chongqing, China; Curitiba, Brazil; Essen/Halle, Germany; Florida, USA; Mexico City, Mexico; Nijmegen, The Netherlands; Paris, France; and Tübingen, Germany) and three collaborating consortia (ESMI, EUROSCA, and READISCA) in accordance with their respective ethics and governance bodies. All data were anonymized and given new subject identifiers prior to aggregation.

Participants with SCA3 were included based on: (1) at least 52 CAG repeats in *ATXN3*,[1] including individuals with and without manifest ataxia and/or (2) genetically confirmed family history of SCA3 with clinical manifestation of disease-consistent ataxia. Ataxia duration was recorded as the time since the patient first recognized their ataxia symptoms. Ataxia severity was quantified using the Scale for Assessment and Rating of Ataxia (SARA).[27] Subjects were excluded on the basis of (1) missing demographic data, (2) poor image quality, or (3) sites without age-matched healthy controls (Supplementary Methods;Fig. S1).

A whole-brain, 3D T_1-weighted structural MRI image was collected for each subject. Imaging protocols varied by site but were consistent between SCA3 and CONT cohorts at each site (Table S1).

Image Processing

All T_1-weighted images were preprocessed as previously described[28] using specialized software for analyzing the cerebellum and cerebrum.[29] First, a cerebellar mask was derived for each image using the SUIT or ACAPULCO[30] algorithms (v0.2.1). The automated masks were visually inspected, with minor segmentation errors corrected manually and major errors resulting in exclusion. Next, cerebellar grey matter (GM) was extracted using the Spatially Unbiased Infratentorial Toolbox (SUIT)[31] v3.2 for SPM12[32] v7771 for MATLAB and DARTEL normalized and resliced into SUIT space; Jacobian modulation was used to ensure that the value assigned to each voxel remained proportional to its original volume. The resulting cerebellar GM images were inspected for normalization errors, and the spatial covariance of these images was calculated and compared across the entire cohort: outliers were visually inspected to determine if rejection was necessary due to processing errors. Finally, the resulting images were spatially smoothed using a Gaussian kernel at a full width at half-maximum (FWHM) of 3 mm.

Because SUIT is optimized for cerebral GM, whole-brain WM and cerebral GM were calculated using the Computational Anatomy Toolbox (CAT12, v12.5)[33] for SPM12. The raw images were bias-field corrected, skull-stripped, then segmented into GM, WM, and cerebrospinal fluid (CSF) partial volumes, from which intracranial volume (ICV) could be calculated. These images were DARTEL registered into Montreal Neurological Institute (MNI) space with Jacobian modulation to maintain volume encoding. The GM image was masked to remove the cerebellum to prevent spatial smoothing of effects between the cerebellum and cerebrum. Finally, both the GM and WM images were smoothed with a 5 mm FWHM Gaussian kernel.

Statistical Analysis

Demographic and clinical analyses were undertaken using R v4.3.3. The distribution of ages in each group was checked for normality using the Shapiro–Wilk test; if at least one group was not normally distributed, the Wilcoxon rank-sum test was used to determine if groupwise differences were significant. Sex was compared between groups using Fisher's exact test.

All image-based statistical analyses were performed using SPM12 in MATLAB. In all cases, heteroscedasticity

was assumed, with final voxel-level inferences estimated with family-wise error (FWE) corrections at the $\alpha = 0.05$ level, using random field theory to account for the large number of multiple comparisons.[34] Only significant clusters with $k \geq 100$ voxels were reported, ensuring robust but conservative inference. Statistical maps showing significant results were then converted to Cohen's d (groupwise analyses) or Pearson's r (correlation analyses) to describe effect sizes.[35,36]

Between-Group Analysis for Disease Effects

Groupwise comparisons between SCA3 and CONT participants were performed using a general linear model (GLM) with factors of Group (2 levels) and Site (11 levels), and covariates ICV and Age. Of these, only Group is a comparison of interest; the remainder are included as nuisance variables. Sex (2 levels) was initially also included as a factor for consideration; however, the effect of its inclusion was negligible (Fig. S2) so it was omitted from the final model.

For interpretative purposes, the voxel-based results were mapped to several anatomical atlases: the Harvard-Oxford cortical and subcortical GM atlases and the Johns Hopkins University cortical WM atlas, as included with FSL[37]; the SUIT cerebellar grey matter and dentate nucleus atlases[38,39]; the van Baarsen cerebellar WM atlas[40]; and the FreeSurfer brainstem atlas.[41] Significant results in the cerebellar GM were additionally mapped onto a multidomain task-based (MDTB) parcellation developed by King et al.[26] to determine correspondence between atrophy and functional regions of the cerebellum.

Clinical Correlations for SCA3 Participants

The spatially-smoothed SCA3 cohort images were adjusted for the effects of healthy aging[42] and site-specific confounds[43] using previously published methodology.[44] Briefly, control subject images were linearly regressed against age, and the slope coefficient of that relationship was used to adjust ataxic subject images to account for healthy aging effects. Site effects were eliminated by subtracting the mean of each site's CONT images from the mean of all CONT images to calculate site-specific volume offset maps, then adjusting each subject image by their site's offset map.

These corrected images were then correlated with ataxia intensity (ie, SARA) and duration, with ICV included as a nuisance covariate. For the pre-ataxic cohort, estimated time to onset was calculated using the methodology of Tezenas du Montcel et al.[45] and included as a negative duration value.

Disease Staging

Cross-sectional analyses were performed on subsets of the SCA3 participant data to visualise disease evolution. The data were subdivided into five groups – pre-ataxic (SARA < 3)[46] and four quartiles of ataxic individuals (separation values: SARA = 8, 11, and 16) – which were then compared with the full CONT cohort using a GLM with ICV as a nuisance covariate. To minimize potential site effects, these analyses were undertaken using the same age- and site-corrected images previously generated for the correlations. Separately, subjects were stratified into high- and low-CAG repeat length groups, and high- and low-ataxia duration groups using the median of each measure (CAG length: 70 repeats; ataxia duration: 9 years) to create a second set of comparisons using the same data.

Cerebrocerebellar Covariance

To better understand the relationship between cerebellar and cerebral disease effects, we undertook a cerebrocerebellar covariance analysis, using the following linear model:

$$Cerebrum \sim Cerebellum + Group + (Cerebellum \times Group) + ICV$$

where *Cerebrum* and *Cerebellum* represent the respective volumes in those regions of the brain, *Group* is a binary variable representing CONT (0) or SCA3 (1), and *ICV* is intracranial volume as a covariate. This model was run separately for GM volume, WM volume, and the two summed together. For this analysis, SUIT-derived cerebellar WM was processed using the same procedure as the cerebellar GM and used in lieu of the CAT12-derived whole-brain WM, while the CAT12-derived WM was cropped to the cerebrum.

As this analysis was intended to examine the extent to which cerebellar and cerebral atrophy are linked, the Cerebellum-by-Group interaction was the regressor of interest: stronger correlations in the SCA3 cohort versus CONT would imply that atrophy in the cerebellum and cerebrum are linked, while a weaker correlation in SCA3 versus CONT would imply that the two are relatively independent.

Results

Demographic and clinical data from the final dataset are summarized in Table 1. The SCA3 and CONT cohorts were age- and sex-matched within each site, and in aggregate showed no significant differences in either sex ($\chi^2 = 0.921$; $P = 0.383$) or age (Wilcoxon $W = 47360.5$, $P = 0.792$).

Volumetric Differences Between SCA3 Participants and Healthy Controls

The GLM comparing SCA3 and CONT participants found numerous areas of significant ($P_{FWE} < 0.05$) atrophy. Those with the greatest effect sizes were observed in

TABLE 1 *Summary of subject demographic and clinical characteristics*

Characteristic	SCA3							CONT		
Site	n	F (%)	Age, years (SD)	Disease duration, years (SD)	CAG repeats, n (SD)	SARA	Pre-ataxic (%)	n	F (%)	Age, years (SD)
Baltimore	11	8 (72.7)	51.6 (10.1)	8.3 (4.5)	70.3 (3.0)	10.8 (5.4)	1 (9.1)	12	8 (66.7)	48.6 (11.8)
Campinas	79	43 (54.4)	48.1 (12.6)	10.4 (7.0)	72.0 (3.7)	13.5 (8.6)	5 (6.3)	82	43 (52.4)	47.5 (11.7)
Chongqing	42	18 (42.9)	41.2 (12.4)	8.4 (4.1)	66.2 (4.3)	10.5 (8.3)	8 (19.0)	55	27 (49.1)	41.9 (13.0)
Curitiba	16	7 (43.8)	44.6 (13.2)	10.8 (7.0)	–[a]	13.4 (5.5)	0 (0.0)	17	8 (47.1)	43.9 (11.9)
ESMI	59	30 (50.8)	48.1 (11.5)	9.5 (5.7)	69.2 (4.1)	9.4 (7.0)	14 (23.7)	21	10 (47.6)	50.0 (13.9)
Essen/Halle	22	11 (50.0)	52.0 (13.9)	13.5 (7.0)	68.2 (4.1)	10.1 (5.3)	3 (13.6)	21	8 (38.1)	51.8 (14.3)
Mexico	16	9 (56.3)	40.3 (12.3)	6.9 (4.7)	72.6 (3.9)	13.3 (7.7)	2 (12.5)	15	7 (46.7)	41.7 (13.3)
Nijmegen	17	8 (47.1)	37.4 (9.6)	–[b]	66.8 (2.9)	1.5 (1.0)	17 (100.0)	8	2 (25.0)	31.3 (8.2)
Paris	20	12 (60.0)	50.9 (11.8)	8.7 (4.5)	68.9 (5.6)	13.0 (7.2)	3 (15.0)	24	13 (54.2)	49.8 (12.8)
READISCA	48	30 (62.5)	43.8 (10.1)	4.8 (4.4)	70.4 (3.6)	4.2 (3.1)	19 (39.6)	12	6 (50.0)	41.3 (7.5)
Tübingen	9	3 (33.3)	40.4 (8.3)	9.0 (5.7)	67.6 (2.4)	3.3 (4.0)	6 (66.7)	9	3 (33.3)	41.0 (9.0)
Total	339	179 (52.8)	45.9 (12.3)	9.2 (6.1)	69.6 (4.4)	9.9 (7.7)	78 (23.0)	276	135 (48.9)	45.6 (12.8)

Abbreviations: SCA3, spinocerebellar ataxia type 3; CONT, controls; n, number of subjects; F, number of female subjects; SD, standard deviation; SARA, Scale for the Assessment and Rating of Ataxia score.
[a]Data not available.
[b]No manifest ataxia subjects.

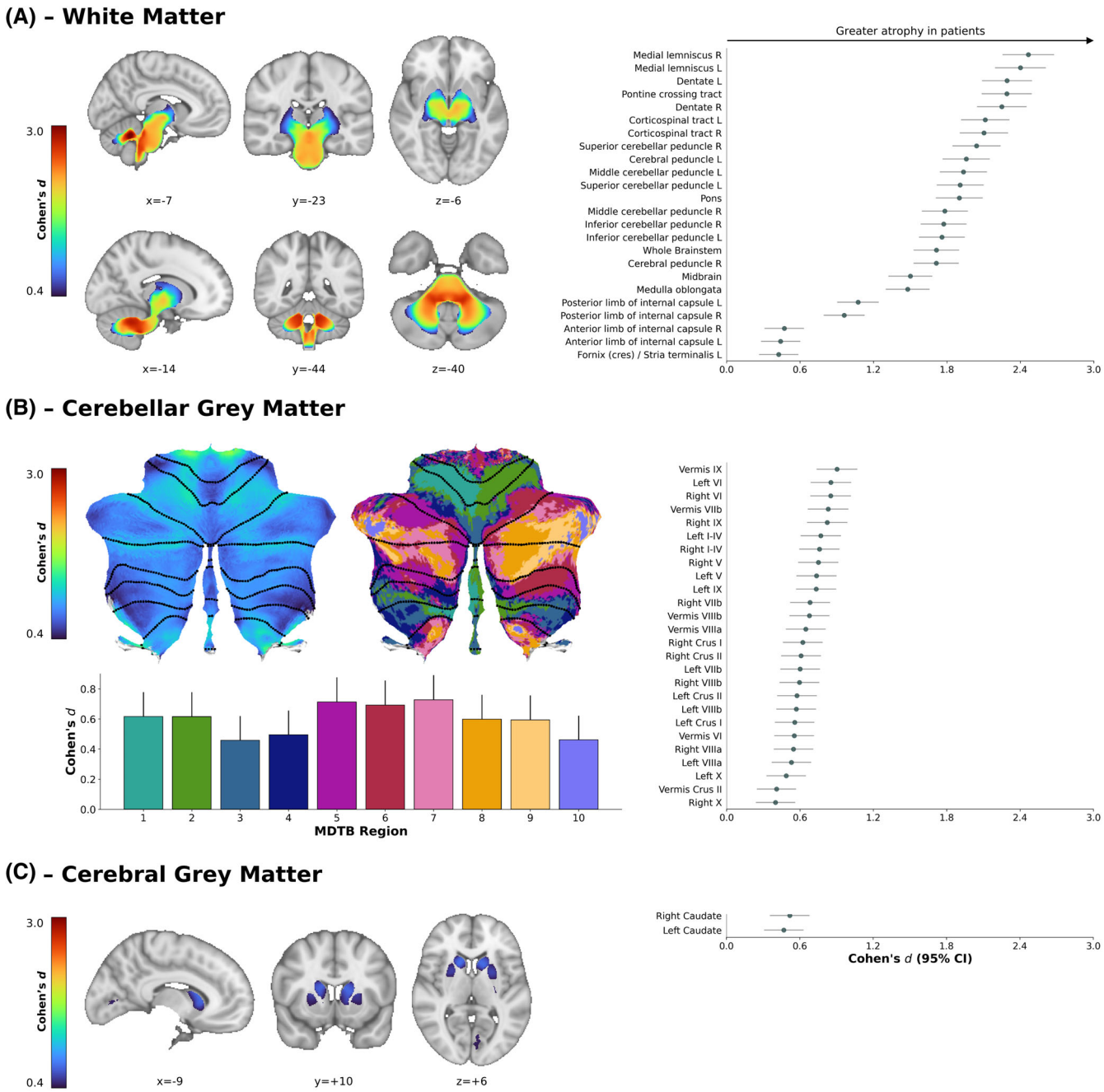

FIG. 1. Volume is greater in controls than spinocerebellar ataxia type 3 (SCA3) participants in (A) white matter, (B) cerebellar grey matter, and (C) cerebral grey matter. Right: Forest plots of significantly affected regions. Panel (B) includes functional map from King et al.[26] with corresponding effect sizes. MDTB, multidomain task-based. [Color figure can be viewed at wileyonlinelibrary.com]

the WM of the brainstem and cerebellum ($d < 1.5$; Fig. 1A), including the medial lemniscus, dentate region, pons, pontine crossing tract, corticospinal tract, and the cerebellar peduncles. Significant but less pronounced atrophy ($0.4 < d < 1.5$) was observed in the midbrain, medulla, and internal capsule. In the cerebellar GM, atrophy at a medium to large effect size was evident in all regions ($d < 1.0$; Fig. 1B), most notably in bilateral Lobule I-IV, Lobule VI, Lobule IX, and Vermis VIIb and IX. In the cerebral GM (Fig. 1C), only the bilateral caudate nuclei and dorsal-anterior putamen were significantly atrophied in SCA3 participants compared with controls.

Analysis of the full dataset, including data from sites with small cohort sizes or no matched healthy controls, replicated these results in addition to focal additional areas of significant cerebral GM atrophy (Fig. S3).

Network Representation of Between-Group Differences

The cerebellar GM results were additionally mapped onto the MDTB functional regions (Fig. 1B). The highest atrophy was observed in MDTB Regions 5–7 ($d \cong 0.7$), which are associated with attention,

executive function, and language/emotional processing. The next tier of atrophy ($d \cong 0.6$) was observed in MDTB Regions 1, 2, 8, and 9; the former two represent motor planning and execution while the latter two represent verbal processing. The weakest atrophy ($d < 0.5$) was observed in regions 3, 4, and 10, which represent a variety of predominantly non-motor skills.

Clinical Correlations in SCA3 Participants

Voxelwise correlations were performed to illustrate how atrophy relates to ataxia duration and ataxia severity as measured by the SARA (Fig. 2, top panel). The significant ($P_{FWE} < 0.05$) correlations with both metrics followed similar trends: large negative correlations with volume ($-0.4 > r > -0.65$) were found in the cerebellar and brainstem WM, while more moderate negative correlations ($-0.25 > r > -0.4$) were observed through much of the cerebellar GM. Correlations with ataxia duration were plotted for a subset of representative regions (Fig. 2, bottom panel): volumes were z-normalized with respect to the CONT cohort as previously described.[12] Consistent with the voxelwise findings, the WM and cerebellar GM regions showed moderate to strong correlations, while the bilateral caudate – which had the strongest atrophy observed in the cerebral GM – did not (Fig. 2, bottom panel). No significant correlations were observed between SARA and cerebral GM volume.

Correlations in the full dataset, without age and site correction, indicated the presence of significant correlations in regions of the cerebral GM (Fig. S4); however, assessing reassessing the main dataset without correction for age and site produced near-identical results, suggesting that these new findings were superfluous; further commentary appears with Figure S5.

Disease Severity Stratification

To characterize the evolution of significant atrophy versus controls ($P_{FWE} < 0.05$) over the course of SCA3, the disease cohort was stratified by SARA score (Fig. 3). Broadly speaking, tissue atrophy becomes more severe as ataxia severity increases, particularly in the brainstem and cerebellum, consistent with the correlation analyses. In cerebellar WM, the spatial extent of the atrophy does not change appreciably across the disease course; however, the severity of the atrophy increases markedly with disease progression. In cerebellar GM, pre-ataxic subjects show limited but significant atrophy, predominantly in the anterior regions, which spreads to the rest of the cerebellum and intensifies in the later stages. When mapped onto the MDTB atlas, the pattern of effect sizes within each stage mirrored that of the full groupwise comparison, indicating that the *pattern* of atrophy is relatively stable across the disease course (Fig. S6). In the cerebral GM, significant atrophy is evident in the striatum at all disease stages, with no evidence of spreading or intensification across stages; this lack of consistent or progressive involvement of cerebral GM matches the full groupwise and clinical correlation results.

We also observed an unusual significant result in the right frontal-orbital cortex in pre-ataxic subjects, which subsequently disappears in the ataxic subjects. This finding also appears in the groupwise analysis of the initial dataset (Fig. S3) but nowhere else. To further explore and validate this observation, we present the stratified data at subsignificance thresholds in Figure S7.

Finally, the results of the CAG repeat length and ataxia duration stratifications are presented in Figure S8, which shows small differences in the spatial extent of significant atrophy versus controls ($P_{FWE} < 0.05$) between the four groups. The greatest atrophic effect size occurs in the cerebellum in the high-CAG, high-duration group.

Cerebrocerebellar Covariance

The linear models representing cerebrocerebellar covariance in GM, WM, and total volume all produced significant fits, with significant main effects of both Group and Cerebellum, as well as Cerebellum × Group interactions. The model thus indicates significant relationships between cerebral and cerebellar volume throughout, but differing magnitudes of these relationships in the CONT and SCA3 groups. This is illustrated in plots of the model fit (Fig. 4), which show diverging linear fits for CONT and SCA3 in all three tissue types, with the linear fit for SCA3 shallower than that of CONT in all cases, indicating reduced cerebro-cerebellar covariance. Detailed model statistics are provided in Table S2.

Discussion

In this multisite MRI study of participants with SCA3 and matched controls, we observed the greatest atrophy in the cerebellar WM and brainstem, with more moderate atrophy occurring across the entirety of the cerebellar GM and parts of the basal ganglia. The overall spatial pattern of atrophy in the cerebellar cortex and brainstem remained consistent with disease progression, although correlations with measures of ataxia severity were strongest in the pons and cerebellar WM. Mapping the cerebellar GM results onto a functional atlas showed that the strongest effects occurred in areas related to motor control, cognitive processing, and emotional regulation. Cerebrocerebellar covariance analysis found reduced covariance in SCA3 participants relative to controls, suggesting that cerebellar atrophy

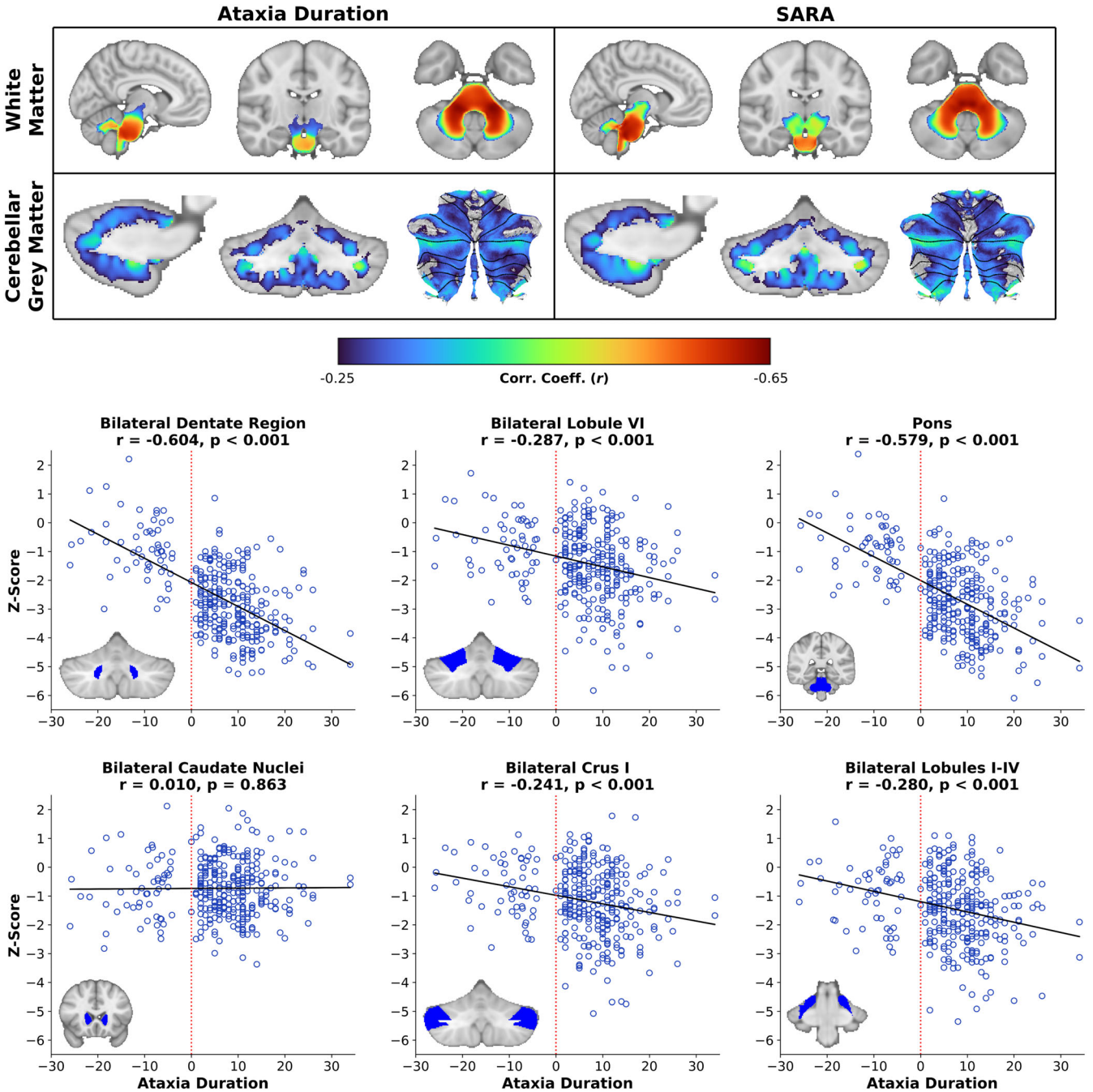

FIG. 2. Correlation analysis results. Top: Voxel maps of significant correlations with ataxia duration and severity. Bottom: Correlations between z-normalized regional volume and ataxia duration, with region locations highlighted in the lower left corner. SARA, Scale for the Assessment and Rating of Ataxia score. [Color figure can be viewed at wileyonlinelibrary.com]

does not occur in parallel with downstream cerebral anatomical changes.

Core Atrophic Signature of SCA3

Brainstem and cerebellar WM atrophy was the predominant characteristic of SCA3 observed here. This finding is consistent with established literature indicating that WM degradation is a common, early, and progressive manifestation of SCA3, occurring prior to the first onset of motor symptoms.[5,12,13] Robust correlations with disease duration and ataxia severity observed in this study are also in line with the established body of longitudinal and cross-sectional studies indicating that atrophy in these core regions worsens as SCA3 progresses.[6,7,9-16,20,21,47,48] Recent studies of cellular mechanisms in murine models have found that oligodendrocyte dysfunction precedes the first loss of motor function, implying that demyelination is a key element

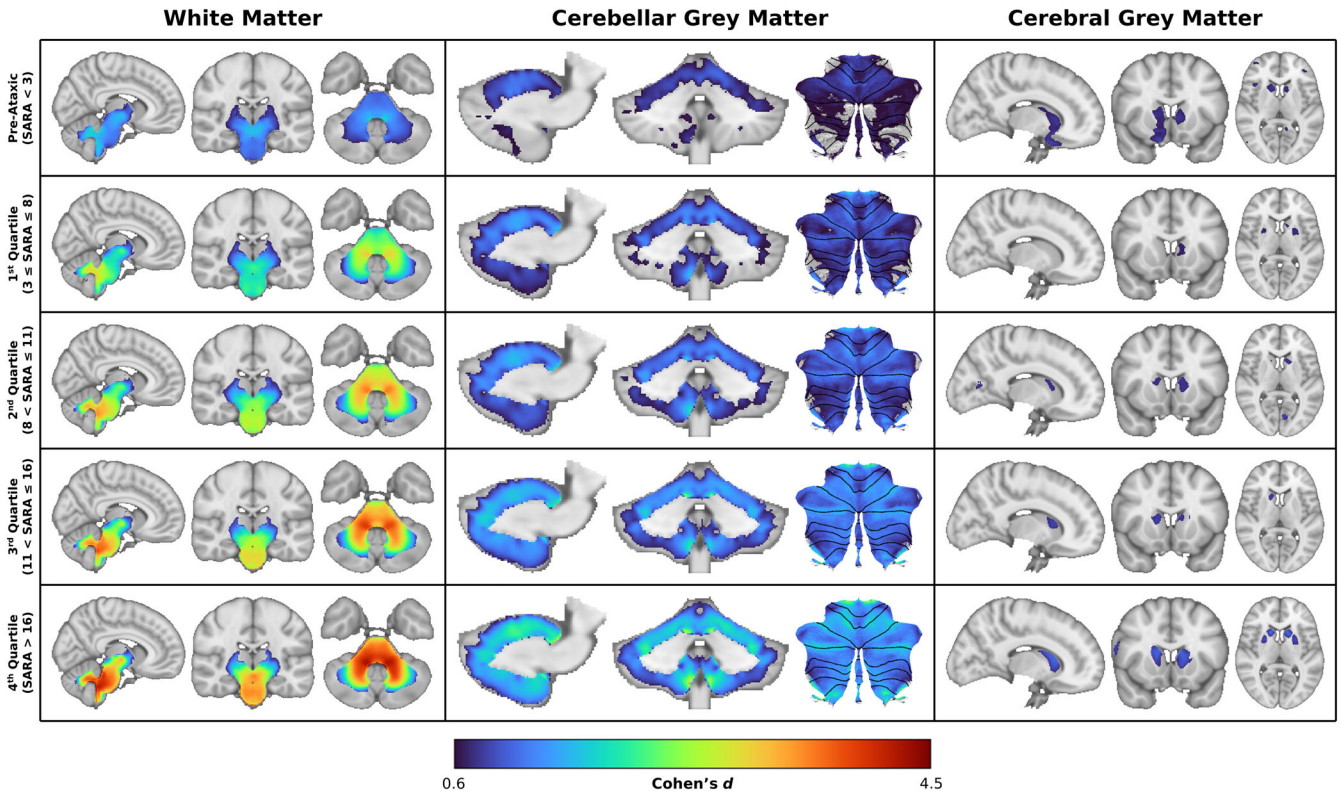

FIG. 3. Voxel maps of significant effects when comparing each ataxia severity stratum to controls. SARA, Scale for the Assessment and Rating of Ataxia score. [Color figure can be viewed at wileyonlinelibrary.com]

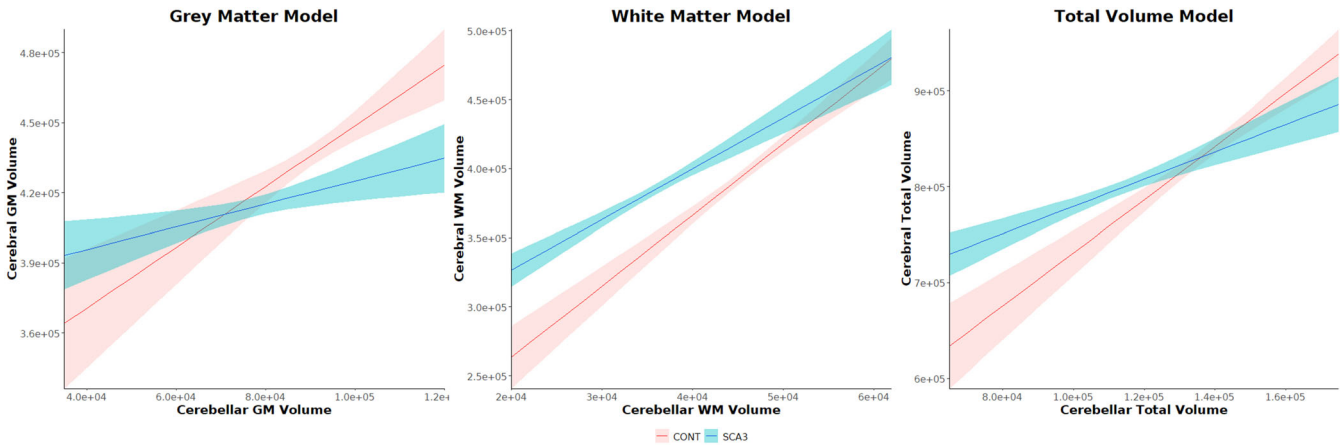

FIG. 4. Fitted linear models with 95% confidence intervals showing uncoupled cerebral and cerebellar atrophy in grey matter (GM) (left), white matter (WM) (middle), and total brain volume (right). [Color figure can be viewed at wileyonlinelibrary.com]

of early WM atrophy in SCA3 and other similar neurodegenerative disorders,[2,49] though this has yet to be demonstrated in humans.

More modest GM atrophy effects were observed across the whole cerebellar cortex, as well as the bilateral caudate and bilateral putamen nuclei, consistent with previous reports.[6,7,12-14,50] Here we show that the anterior lobe and superior aspects of the posterior lobe (Lobules I–VI) are impacted first in pre-ataxic individuals, followed by Lobule IX and the remainder of the superior posterior lobe (Lobule VII), then finally Lobules VIIIa/b and X. The relative magnitude of atrophy in each region follows the same pattern across all disease stages. Correlations with disease severity and duration were evident across the cerebellar cortex, particularly in areas neighbouring WM, suggesting the potential for partial volume effects to be driving some of this anatomical variability.

Functional Mapping in the Cerebellum

Mapping the cerebellar GM atrophy onto a task-based functional map[26] showed varying magnitudes of atrophy across different functional regions of the cerebellar cortex. Although all regions were impacted, a pattern emerged whereby atrophy was greater in functional regions associated with motor planning/execution, attention, and emotional processing, versus regions associated with working memory, sematic/episodic memory, action observation, and saccades. This observation is concordant with the known clinical features of SCA3, including both motor ataxia and a high prevalence of CCAS,[18,19] which is defined by abnormalities in executive function, language processing, visuospatial cognition, and affective regulation.[17]

Inconsistent Evidence of Cerebral and Subcortical Involvement

While the core regions of SCA3 atrophy are consistent across studies, there is less agreement about which parts of the cerebral WM, if any, are affected. Here, we found that WM atrophy extended to the internal capsule and peri-thalamic regions. By contrast, using diffusion tensor imaging, Rezende et al.[13] observed lower fractional anisotropy relative to controls, implying a loss of WM integrity, across much of the subcortical WM. Other studies have reported reduced integrity in structures such as the forceps major and minor,[21] inferior and superior longitudinal fasciuli,[10,21] thalamus,[14,16] anterior and posterior thalamic radiations,[13,21] corona radiata,[7,13,14] and corpus callosum[13] in their respective SCA3 cohorts. These differing findings may be due to the generally greater sensitivity of diffusion MRI metrics to WM microstructural differences versus the volumetric approach taken here.[16,50]

We did not find robust evidence of consistent cerebral cortical GM atrophy in individuals with SCA3, even at late disease stages as previously reported.[13] Notably, however, at reduced, non-significant statistical thresholds, trend-level findings with small effect sizes (ie, $0.3 \leq d \leq 0.5$) are observed (Fig. S7), suggesting mild reductions of volume in areas of the cerebral cortex. That said, there was no consistent anatomical pattern, nor clear evidence of progression of these subthreshold effects across the subgroups of our stratified analysis. With respect to subcortical GM, we observed that atrophy in the striatum appears to be an early, but non-progressive, feature of SCA3. While this is inconsistent with some earlier reports suggesting that striatal atrophy is progressive in the pre-ataxic and/or ataxic stages,[6,14] at least one other study has found no significant difference between pre-ataxic and ataxic subjects.[12]

Taken together, these findings suggest that while individuals with SCA3 are more vulnerable to cerebral degeneration than the general population, there remains extensive individual variability in location and magnitude. Further research will be necessary to determine whether clinical phenomenology and disease course differ in individuals with versus without cerebral involvement.

Cerebrocerebellar Correlational Analysis

To further investigate the relationship between cerebral and cerebellar atrophy we performed a structural covariance analysis. We observed strong covariance between cerebral and cerebellar volume in controls, particularly in the WM. Attenuation of this relationship in individuals with SCA3 suggests that volume loss in the cerebellum occurs relatively independently of any cerebral changes. This result provides further weight to our conclusion that the consistent profile of cerebellar volume loss in those with SCA3 is not reflected in cerebral pathology.

Limitations

Our dataset is rich in T_1-weighted images and standard clinical measures of ataxia severity, duration, and genetic load. Conversely, we lack the cognitive testing or functional MRI data that would allow more definitive insights into the relationship between cerebellar changes and non-motor symptoms. We also lack consistent data on specific non-ataxic clinical signs such as spasticity[51] and parkinsonism[52] due to the retrospective, multisite nature of this study (eg, differing site protocols and data protection regulations). More in-depth clinical phenotyping would provide opportunities to unravel the natural heterogeneity of SCA3, including distinguishing the neurobiology of clinical subtypes.[1,4,5]

Diffusion-weighted MRI would also allow for a more sensitive assessment of WM microstructural integrity versus our current volume-based techniques. Additionally, while the large SCA3 cohort size of our dataset allows for stratification based on disease severity, we recognize that cross-sectional stratification analysis is not a perfect proxy for a true longitudinal study. Finally, while cerebrocerebellar structural covariance analyses provide an indication of the relative coupling of cerebral and cerebellar degeneration, a true assessment of cerebrocerebellar connectivity changes in SCA3 will require functional and/or microstructural imaging approaches.[3]

Conclusions

In this large, multisite study, we demonstrate that the core neuroanatomical changes in participants with

SCA3 occur in a relatively stable pattern of brainstem and cerebellar atrophy that is progressive in magnitude but not spatial extent, particularly after the onset of ataxia symptoms. This atrophy pattern maps onto functional divisions of the cerebellum that are consistent with the motor and non-motor features of the disease. Finally, we show that this core cerebellar atrophy is not directly mirrored by downstream cerebral changes and that cerebral volume loss, if present, may have higher individual variability. These findings expand our fundamental understanding of the neuroanatomy of SCA3. ■

Author Roles: (1) Research Project: A. Conception, B. Organization, C. Execution; (2) Statistical Analysis: A. Design, B. Execution, C. Review and critique; (3) Manuscript: A. Writing of the First Draft, B. Review and Critique.
J.W.R.: 1C, 2B, 2C, 3A, 3B.
I.A.: 1C, 3B.
D.J.A.: 1C, 3B.
T.A.: 1C, 3B.
B.B.: 1C, 3B.
F.C.: 1C, 3B.
X.C.: 1C, 3B.
G.C.: 1C, 3B.
L.C.: 1C, 3B.
A.De.: 1C, 3B.
I.D.: 1C, 3B.
A.Du.: 1C, 3B.
J. F.: 1C, 3B.
J. F.-R.: 1C, 3B.
M.F.: 1C, 3B.
M.C.F.: 1C, 3B.
S.L.G.: 1C, 3B.
S.H.: 1C, 3B.
T.K.: 1C, 3B.
C.L.: 1C, 3B.
J.L.: 1C, 3B.
A.R.M.M.: 1C, 3B.
S.E.O.: 1C, 3B.
C.U.O.: 1C, 3B.
G.Ö.: 1C, 3B.
H.P.: 1C, 3B.
J.L.P.: 1C, 3B.
K.R.: 1C, 3B.
T.J.R.R.: 1C, 3B.
M.S.: 1C, 3B.
H.A.G.T.: 1C, 3B.
S.I.T.: 1C, 3B.
P.M.T.: 1C, 3B.
D.T.: 1C, 3B.
D.V.: 1C, 3B.
B.v.d.W: 1C, 3B.
J.v.G.: 1C, 3B.
X.W.: 1C, 3B.
P.W.: 1C, 3B.
S.H.Y.: 1C, 3B.
I.H.H.: 1A, 1B, 1C, 2A, 2B, 2C, 3B.
C.R.H.C.: 1A, 1C, 2A, 2B, 2C, 3B.

Acknowledgments: The authors would like to acknowledge the contributions of Victor Gadelha, Hellen Della-Justina, Salmo Raskin, Arnolfo de Carvalho Neto, B.M. and C.W.W. Girard, and Elodie Petit. Several authors of this publication are members of the European Reference Network for Rare Neurological Diseases (ERN-RND). Some data and/or research tools used in the preparation of this article were obtained from the National Institute of Mental Health (NIMH) Data Archive (NDA). NDA is a collaborative informatics system created by the National Institutes of Health (NIH) to provide a national resource to support and accelerate research in mental health. This article reflects the views of the authors and may not reflect the opinions or views of the NIH or of the submitters submitting original data to NDA. Additional collaborating authors represented by the ESMI MR Study Group: Heike Jacobi, MD, PhD.; Jeroen de Vries, MD; Paola Giunti, MD, PhD; and Hector Garcia-Moreno, MD, PhD. Additional collaborating authors represented by the EUROSCA MR Study Group include Caterina Mariotti, MD; Maria Julia Rakowicz, PhD; and Ludger Schöls, MD, PhD.

Financial Disclosures of All Authors (for the Past 12 Months): Additional funding has been provided by the following sources: the Ministry of Culture and Science of the State of North Rhine-Westphalia to J.F, as a Principal Investigator (PI) of the iBehave Network; the National Institute of Biomedical Imaging and Bioengineering (NIBIB) grant P41 EB027061 and the Institutional Center Cores for Advanced Neuroimaging award P30 NS076408 and grant S10 OD017974, all to the Center for Magnetic Resonance Research, Minneapolis, which employs I.A. and G. Ö.; the National Institute for Health Research (NIHR), University College London Hospitals (UCLH) Biomedical Research Centre, and CRN North Thames, to Paola Giunti; and CureSCA3, to Paola Giunti specifically in support of Hector Garcia-Moreno.

Data Availability Statement

READISCA data are available at https://doi.org/10.15154/3xeb-fz42. All code and data processing instructions are available at https://github.com/HardingLab/enigma-ataxia. Other ENIGMA collaborator data may be requested for further research purposes through a secondary data use proposal submitted to the ENIGMA-Ataxia working group (http://enigma.ini.usc.edu/ongoing/enigma-ataxia).

References

1. Rüb U, Schöls L, Paulson H, et al. Clinical features, neurogenetics and neuropathology of the polyglutamine spinocerebellar ataxias type 1, 2, 3, 6 and 7. Prog Neurobiol 2013;104:38–66.
2. Schuster KH, Putka AF, HS ML. Pathogenetic mechanisms underlying spinocerebellar ataxia type 3 are altered in primary oligodendrocyte culture. Cells 2022;11(16):2615.
3. Yap KH, Abdul Manan H, Yahya N, Azmin S, Mohamed Mukari SA, Mohamed Ibrahim N. Magnetic resonance imaging and its clinical correlation in spinocerebellar ataxia type 3: a systematic review. Front Neurosci 2022;16:859651.
4. Sun Y-M, Lu C, Wu Z-Y. Spinocerebellar ataxia: relationship between phenotype and genotype – a review. Clin Genet 2016;90(4):305–314.
5. Lindsay E, Storey E. Cognitive changes in the spinocerebellar ataxias due to expanded polyglutamine tracts: a survey of the literature. Brain Sci 2017;7(7):83.
6. Reetz K, Costa AS, Mirzazade S, et al. Genotype-specific patterns of atrophy progression are more sensitive than clinical decline in SCA1, SCA3 and SCA6. Brain 2013;136(3):905–917.
7. Adanyeguh IM, Perlbarg V, Henry P-G, et al. Autosomal dominant cerebellar ataxias: imaging biomarkers with high effect sizes. Neuroimage Clin 2018;19:858–867.
8. Jacobi H, Tezenas du Montcel S, Romanzetti S, et al. Conversion of individuals at risk for spinocerebellar ataxia types 1, 2, 3, and 6 to manifest ataxia (RISCA): a longitudinal cohort study. Lancet Neurol 2020;19(9):738–747.
9. de Oliveira CM, Leotti VB, Polita S, et al. The longitudinal progression of MRI changes in pre-ataxic carriers of SCA3/MJD. J Neurol 2023;270(9):4276–4287.
10. Rezende TJR, Petit E, Park YW, et al. Sensitivity of advanced magnetic resonance imaging to progression over six months in early spinocerebellar ataxia. Mov Disord 2024;39(10):1856–1867.
11. Berger M, Garcia-Moreno H, Ferreira M, et al. Progression of biological markers in spinocerebellar ataxia type 3: longitudinal analysis of prospective data from the ESMI cohort. Lancet Reg Health Eur 2025;55:101339.
12. Faber J, Schaprian T, Berkan K, et al. Regional brain and spinal cord volume loss in spinocerebellar ataxia type 3. Mov Disord 2021;36(10):2273–2281.
13. Rezende TJR, de Paiva JLR, Martinez ARM, et al. Structural signature of SCA3: from presymptomatic to late disease stages. Ann Neurol 2018;84(3):401–408.

14. Chandrasekaran J, Petit E, Park YW, et al. Clinically meaningful magnetic resonance endpoints sensitive to preataxic spinocerebellar ataxia types 1 and 3. Ann Neurol 2023;93(4):686–701.
15. Faber J, Berger M, Wilke C, et al. Stage-dependent biomarker changes in spinocerebellar ataxia type 3. Ann Neurol 2024;95(2): 400–406.
16. Guimarães RP, D'Abreu A, Yasuda CL, et al. A multimodal evaluation of microstructural white matter damage in spinocerebellar ataxia type 3. Mov Disord 2013;28(8):1125–1132.
17. Schmahmann JD, Sherman JC. The cerebellar cognitive affective syndrome. Brain 1998;121(4):561–579.
18. Yap KH, Kessels RPC, Azmin S, van de Warrenburg B, Mohamed Ibrahim N. Neurocognitive changes in spinocerebellar ataxia type 3: a systematic review with a narrative design. Cerebellum 2022;21(2): 314–327.
19. Selvadurai LP, Schmahmann JD, Harding IH. Clinical cerebellar neuroscience: cognitive functioning in spinocerebellar ataxias: an update and future directions. Curr Opin Behav Sci 2024;55:101343.
20. Hernandez-Castillo CR, King M, Diedrichsen J, Fernandez-Ruiz J. Unique degeneration signatures in the cerebellar cortex for spinocerebellar ataxias 2, 3, and 7. Neuroimage Clin 2018;20: 931–938.
21. Meira AT, Arruda WO, Ono SE, et al. Analysis of diffusion tensor parameters in spinocerebellar ataxia type 3 and type 10 patients. Parkinsonism Relat Disord 2020;78:73–78.
22. Testa C, Laakso MP, Sabattoli F, et al. A comparison between the accuracy of voxel-based morphometry and hippocampal volumetry in Alzheimer's disease. J Magn Reson Imaging 2004;19(3):274–282.
23. Douaud G, Gaura V, Ribeiro M-J, et al. Distribution of grey matter atrophy in Huntington's disease patients: a combined ROI-based and voxel-based morphometric study. Neuroimage 2006;32(4): 1562–1575.
24. Cui X, Li L, Yu L, et al. Gray matter atrophy in Parkinson's disease and the parkinsonian variant of multiple system atrophy: a combined ROI-and voxel-based morphometric study. Clinics 2020;75: e1505.
25. Seyedi S, Jafari R, Talaei A, et al. Comparing VBM and ROI analyses for detection of gray matter abnormalities in patients with bipolar disorder using MRI. Middle East Curr Psychiatry 2020;27 (1):69.
26. King M, Hernandez-Castillo CR, Poldrack RA, Ivry RB, Diedrichsen J. Functional boundaries in the human cerebellum revealed by a multi-domain task battery. Nat Neurosci 2019;22(8): 1371–1378.
27. Schmitz-Hübsch T, Tezenas du Montcel S, Baliko L, et al. Scale for the assessment and rating of ataxia. Neurology 2006;66(11):1717–1720.
28. Kerestes R, Han S, Balachander S, et al. A standardized pipeline for examining human cerebellar grey matter morphometry using structural magnetic resonance imaging. J Vis Exp 2022;180:63340.
29. Hernandez-Castillo CR. Methods for cerebellar imaging: cerebellar subdivision. Curr Opin Behav Sci 2023;53:101302.
30. Han S, Carass A, He Y, Prince JL. Automatic cerebellum anatomical parcellation using U-net with locally constrained optimization. Neuroimage 2020;218:116819.
31. Diedrichsen J. A spatially unbiased atlas template of the human cerebellum. Neuroimage 2006;33(1):127–138.
32. Ashburner J. Computational anatomy with the SPM software. Magn Reson Imaging 2009;27(8):1163–1174.
33. Gaser C, Dahnke R, Thompson PM, Kurth F, Luders E. Alzheimer's disease neuroimaging initiative. CAT – a computational anatomy toolbox for the analysis of structural MRI data. *bioRxiv* 2023: 2022.06.11.495736.
34. Brett M, Penny W, Kiebel S. Introduction to random field theory. In: Ashburner J, Friston KJ, Penny W, eds. Human Brain Function. Elsevier Academic Press; 2nd ed. London, UK; 2003.
35. Nakagawa S, Cuthill IC. Effect size, confidence interval and statistical significance: a practical guide for biologists. Biol Rev 2007; 82(4):591–605.
36. Hedges LV, Olkin I. Statistical Methods for Meta-Analysis. Orlando, FL, USA: Academic Press Inc.; 1985.
37. Jenkinson M, Beckmann CF, Behrens TEJ, Woolrich MW, Smith SM. FSL. Neuroimage 2012;62(2):782–790.
38. Diedrichsen J, Balsters JH, Flavell J, Cussans E, Ramnani N. A probabilistic MR atlas of the human cerebellum. Neuroimage 2009; 46(1):39–46.
39. Diedrichsen J, Maderwald S, Küper M, et al. Imaging the deep cerebellar nuclei: a probabilistic atlas and normalization procedure. Neuroimage 2011;54(3):1786–1794.
40. van Baarsen KM, Kleinnijenhuis M, Jbabdi S, Sotiropoulos SN, Grotenhuis JA, van Cappellen van Walsum AM. A probabilistic atlas of the cerebellar white matter. Neuroimage 2016;124: 724–732.
41. Fischl B. FreeSurfer. Neuroimage 2012;62(2):774–781.
42. Matsuda H. Voxel-based morphometry of brain MRI in normal aging and Alzheimer's disease. Aging Dis 2013;4(1):29–37.
43. Jovicich J, Czanner S, Han X, et al. MRI-derived measurements of human subcortical, ventricular and intracranial brain volumes: reliability effects of scan sessions, acquisition sequences, data analyses, scanner upgrade, scanner vendors and field strengths. Neuroimage 2009;46(1):177–192.
44. Harding IH, Chopra S, Arrigoni F, et al. Brain structure and degeneration staging in Friedreich ataxia: magnetic resonance imaging volumetrics from the ENIGMA-Ataxia working group. Ann Neurol 2021;90(4):570–583.
45. Tezenas du Montcel S, Durr A, Rakowicz M, et al. Prediction of the age at onset in spinocerebellar ataxia type 1, 2, 3 and 6. J Med Genet 2014;51(7):479–486.
46. Jacobi H, Reetz K, Tezenas du Montcel S, et al. Biological and clinical characteristics of individuals at risk for spinocerebellar ataxia types 1, 2, 3, and 6 in the longitudinal RISCA study: analysis of baseline data. Lancet Neurol 2013;12(7):650–658.
47. Kang J-S, Klein JC, Baudrexel S, Deichmann R, Nolte D, Hilker R. White matter damage is related to ataxia severity in SCA3. J Neurol 2014;261(2):291–299.
48. Hernandez-Castillo CR, Diaz R, Campos-Romo A, Fernandez-Ruiz J. Neural correlates of ataxia severity in spinocerebellar ataxia type 3/Machado-Joseph disease. Cerebellum Ataxias 2017;4(1):7.
49. Schuster KH, Zalon AJ, Zhang H, et al. Impaired oligodendrocyte maturation is an early feature in SCA3 disease pathogenesis. J Neurosci 2022;42(8):1604–1617.
50. de Rezende TJR, D'Abreu A, Guimarães RP, et al. Cerebral cortex involvement in Machado-Joseph disease. Eur J Neurol 2015; 22(2):277.
51. Ye ZX, Xu HL, Chen NP, et al. Disease progression and multiparametric imaging characteristics of spinocerebellar ataxia type 3 with spastic paraplegia. Neurol Genet 2024;10(3):e200162.
52. Schöls L, Reimold M, Seidel K, et al. No parkinsonism in SCA2 and SCA3 despite severe neurodegeneration of the dopaminergic substantia nigra. Brain 2015;138(11):3316–3326.

Supporting Data

Additional Supporting Information may be found in the online version of this article at the publisher's web-site.